Coherent Water Window X Ray by Phase-Matched High-Order Harmonic Generation in Neutral Media

Eiji J. Takahashi,* Tsuneto Kanai, Kenichi L. Ishikawa, Yasuo Nabekawa, and Katsumi Midorikawa

Extreme Photonics Research Group, RIKEN Advanced Science Institute, 2-1 Hirosawa, Wako, Saitama 351-0198, Japan

(Received 24 July 2008; published 15 December 2008)

We demonstrate the generation of a coherent water window x ray by extending the plateau region of high-order harmonics under a neutral-medium condition. The maximum harmonic photon energies attained are 300 and 450 eV in Ne and He, respectively. Our proposed generation scheme, combining a 1.6 μm laser driver and a neutral Ne gas medium, is efficient and scalable in output yields of the water window x ray. Thus, the precept of the design parameter for a single-shot live-cell imaging by contact microscopy is presented.

DOI: 10.1103/PhysRevLett.101.253901 PACS numbers: 42.65.Ky, 32.30.Rj, 41.50.+h, 42.50.Hz

The realization of a powerful coherent x-ray source has been the dream of researchers of laser physics and photonics. In particular, the spectral range between the *K*-absorption edges of carbon (284 eV) and oxygen (543 eV), which is called the *water window*, is attractive for high-contrast biological imaging. This spectral range has been one of the most important grails in the research and development of coherent x-ray sources. An intense ultrafast water window x-ray pulse would allow us to capture images of live cells by instantaneously halting their motion, preserving structural information that is lost in the sample's preparation process for electron microscopy.

Thus far, the most practical source of coherent x rays has been synchrotron radiation produced by an accelerator. Images of live cells, however, cannot be captured without freezing the sample even using the world's largest synchrotron radiation facility due to its low instantaneous power. On the other hand, an alternative approach of high-order harmonic generation (HHG) using a tabletop laser system has been investigated over the past ten years for generating coherent water window x rays [1,2]. HHG provides highly coherent ultrafast x-ray pulses and even enables the creation of a single burst [3–5] or a train of attosecond pulses [6,7]. Although the generation of a large amount of photon flux with below 100 eV region by phase-matched HHG has been reported [8], the output photon flux at about 300 eV is still less than approximately 10^3 photons/shot with a conversion efficiency (CE) of less than 10^{-10} [1,2]. This is mainly due to phase mismatch induced by *plasma* free electrons, because a high intensity greater than the ionization threshold is required for 0.8 μm Ti:sapphire laser driving.

Here, we show the efficient generation of a coherent x-ray high-order harmonic (HH) in the water window region using an IR driving laser and a *neutral* (nonionized) [9] rare-gas medium. Our proposed procedure for generating the water window x ray is efficient and scalable in output yield, which provides us with the HH parameters required for the imaging of live cells. First, we briefly explain our proposed scheme, combining an IR laser pulse and neutral media.

From a theoretical point of view, the maximum photon energy of HHG is approximately given by $E_{\mathrm{cutoff}}\,[\mathrm{eV}] = I_p + 3.17U_p$ (cutoff low), where I_p is the binding energy of the electrons and $U_p\,[\mathrm{eV}] = 9.38 \times 10^{-14} I\,[\mathrm{W/cm^2}] \times (\lambda_0\,[\mu\mathrm{m}])^2$ is the electron quiver energy (ponderomotive energy). This formula can be explained in terms of the framework of the semiclassical so-called three-step model [10]. A conventional approach to extending the harmonic cutoff is to use very high laser intensity, since the ponderomotive energy is proportional to the pump laser intensity. As the efficiency of harmonic generation is, however, limited by the dephasing of the atomic dipole oscillators and the plasma defocusing of the laser pulse, the CE rapidly decreases when the laser intensity exceeds the ionization threshold of a target gas medium. To overcome this ionization-induced phase mismatch, quasiphase matching (QPM) [11–14] or nonadiabatic self-phase matching (NSPM) [15] has been proposed for efficient harmonic generation from ionized gases. Here, the scalability of HHG is of paramount importance for the development of useful light sources. The scalability of QPM to higher photon energies is limited by the structure of modulation periods. Also, the controllability of the phase-matching condition is unsatisfactory for QPM. Since, as for NSPM, phase matching is fulfilled automatically, external human control is impossible.

An alternative possible approach to extending the harmonic cutoff is to use a longer-wavelength laser for the driving field [16]. Recently, Yakovlev *et al.* [17] theoretically predicted several important advantages of using longer laser wavelengths: conversion efficiency can be improved, and isolated attosecond pulses can be extracted from plateau harmonics, and so on. Harmonic spectra are calculated by the direct numerical solution of the three-dimensional time-dependent Schrödinger equation (TDSE) in the single-active-electron approximation. This TDSE code has been reported and validated in previous

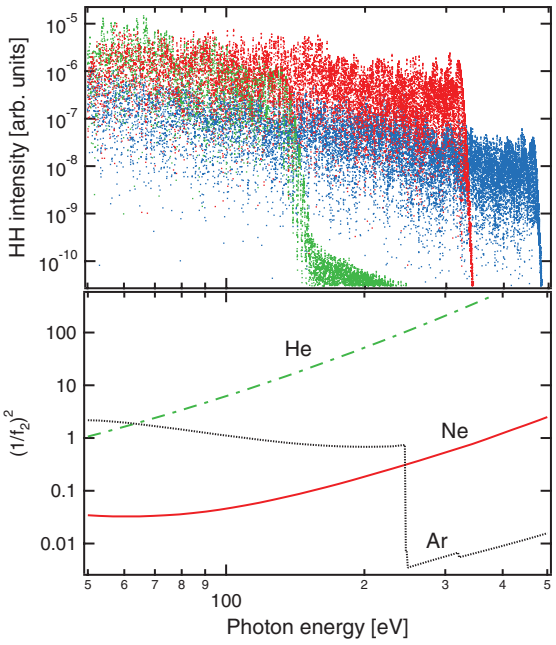

FIG. 1 (color). Calculated harmonic spectra and effect of medium's absorption. The green profile in the top panel depicts the calculated HH spectrum generated in He using a 35 fs, 0.8 μm pulse with an intensity of 5.5×10^{14} W/cm^2. Because the ionization rate is fixed to less than 1%, the cutoff harmonic energy barely attains 150 eV. The red and blue profiles in the top panel show the calculated HH spectra generated by 35 fs, 1.6 μm pulse with an intensity of 4×10^{14} W/cm^2 in Ne and 6×10^{14} W/cm^2 in He, respectively. The bottom panel shows the evolution of the square of the reciprocal of the imaginary component f_2 for three different gases [32], which indicates the effect of absorption.

studies [18–20]. As shown in the top panel of Fig. 1, it is obvious that the HH photon energy extends significantly into the water window region despite the neutral-medium condition when the 1.6 μm laser is employed. On the other hand, when the wavelength of a Ti:sapphire laser is employed, the water window x ray is not generated from a neutral medium. Moreover, since neutral media enable us to adopt a *right* phase-matching [21] technique without QPM and/or NSPM, we can apply an energy-scaling procedure that is well established using a loosely focused beam [8]. On this phase-matching technique, the phase mismatch is fully corrected by adjusting the gas pressure and therefore it is fundamentally more efficient than QPM in the same interaction length.

When the phase-matching condition is satisfied, the amplitude A_q of the qth harmonic taking into account the absorption effect of the medium is given by [21] $\frac{dA_q}{dz} = N_0 d(q\omega_0) \exp(\frac{i\pi z}{L_{\rm coh}}) \exp[-(\frac{L_{\rm med}-z}{2L_{\rm abs}})]$, end equation where $L_{\rm coh} = \pi/\Delta k$ is the coherence length and $\Delta k = k_q - qk_0$ is the total phase mismatch between the HH field and the atomic dipole. The absorption length $L_{\rm abs}$ for the given harmonic corresponds to $\lambda_0/4\pi q\beta$. β is the absorptive parameter of the complex refractive index [22], given by $\beta = \frac{N_0 r_e \lambda_0^2}{2\pi q^2} f_2(\omega)$. The number of qth harmonic photons on the axis per unit of time and area, N_q, is obtained by spatially integrating the harmonic amplitude A_q. In a loosely focusing geometry of a pump pulse, the Gouy phase, the neutral gas dispersion, and the plasma dispersion of the medium are the phase-matching factors. Even when $L_{\rm coh}$ ($\Delta k \sim 0$) is infinite, the HH emission saturates when $L_{\rm med}$ is longer than $3L_{\rm abs}$. Under this absorption limited condition (ALC), the net HH energy yield is proportional to the following expression [8]: $N_q \sim S_{\rm spot}(PL_{\rm med})^2 L_{\rm abs}^2 \sim S_{\rm spot}/f_2^2(\omega)$, where $S_{\rm spot}$ is the spot area of the pump pulse at the focusing point, which corresponds to πw_0^2, w_0 is the spot size and P is the target gas pressure. The above equation indicates that the HH yield is increased by increasing the HH emission size under the optimized phase-matching condition and is also proportional to $(1/f_2)^2$.

To attain efficient HHG, the above absorption feature of a harmonic medium should be noted. In a broad plateau region of nearly constant harmonic intensity, the HH spectrum shape reflects the absorption feature of the medium under the ALC. Although a large extension of the cutoff wavelength of HHG using Ar and a 2.0 μm driving pulse has been reported recently [23], Ar gas has a large absorption coefficient in the water window region, as shown in the bottom panel of Fig. 1. For efficient HHG in the water window region, He and Ne gases are advantageous compared with Ar due to their lower absorption. However, since He has exceptionally small effective nonlinearity, Ne is expected to be the most practical gas for efficiently generating HH in the water window region. The driving wavelength of 2.0 μm is also not always optimum because the HH yield rapidly decreases with increasing driving wavelength [20,24]. Consequently, we consider that the shortest laser wavelength at which the water window HH is generated from neutral Ne gas is optimum for the driving laser.

High-energy IR pulses [25] are produced by two-stage optical parametric amplification at a repetition rate of 10 Hz. The IR pulses are focused using a $f = 250$ mm CaF_2 lens and are delivered into the target chamber through a thin CaF_2 window. The target gas is supplied by a 2-mm-diameter synchronized supersonic gas jet operating at 10 Hz. The generated harmonics illuminate a slit of the spectrometer, which is placed 0.5 m from the gas jet position. A flat-field grating relays the image of the slit to a microchannel plate (MCP), where it is spectrally resolved along the horizontal axis. Here, we use two types of concave grating to measure the broadband wavelength region from 50 to 500 eV. One is specifically designed to cover the 50–200 eV photon energy range with a grazing incident angle of 3° and has a nominal groove number of 1200 grooves/mm with a gold surface; the other is designed to cover the 200–500 eV photon energy range with a grazing incident angle of 1.3° and has a nominal groove number of 2400 grooves/mm with a gold surface [26].

Figure 2 shows the measured Ne HH spectra driven by a 1.55 μm laser pulse at a focusing intensity of 3.5×10^{14} W/cm^2, at which the ionization rate was estimated to be approximately 0.35% from the Ammosov-Delone-Krainov ionization theory [27]. The pump energy was set at 2.2 mJ. Note that the vertical axis of HH intensity is plotted with a linear scale. The measured harmonic spectrum gradually increases up to 250 eV, which is in strong contrast to the previously reported HH spectra in the water window region [1,2,11–14,28]. To evaluate the intensity distribution of the lower harmonics, we changed the spectrometer's grating from 2400 to 1200 grooves/mm. The HH intensity (dotted blue profile in Fig. 2) with the 1200 grooves/mm grating exhibits a broad plateau up to 150 eV. In contrast, the HH intensity rapidly increases above 150 eV, which agrees with the spectrum obtained from the grating with 2400 grooves/mm, then it starts to decrease at 170 eV because of the low diffraction efficiency of the 1200 grooves/mm grating above 170 eV. The HH yield is optimized by adjusting the focusing point and by varying the backing pressure of the gas jet. The HH yield gradually increases as the gas pressure increases, which shows a quadratic dependence of the harmonic yield as a function of gas backing pressure. The HH intensity above the carbon K edge (284 eV) is found to be maximum at a backing pressure of approximately 20 atm with a Gaussian-like spatial profile. By using the configuration parameter of supersonic gas get [29], the effective gas pressure at the interaction region is estimated to be approximately 580 Torr. At the 250 eV photon energy, Gouy phase and gas dispersion are evaluated to be 360 cm^{-1} from the spot size of pump pulse and 615 cm^{-1} from backing pressure, respectively. Also, plasma dispersion is calculated to be 980 cm^{-1} at the 0.35% ionization. To compensate the total phase mismatch, the pump pulse is focused after the gas jet, at which the Gouy phase has a minus sign. The coherence length and absorption length are estimated to be approximately 0.6 and 0.085 cm at the 250 eV HH, respectively. Therefore, our condition almost satisfies the optimized phase-matching condition. The solid red curve in Fig. 2 shows the evolution of $(1/f_2)^2$ as a function of HH photon energy. As expected, the HH intensity increases with increasing $(1/f_2)^2$ up to 250 eV. Above 250 eV, the HH intensity decreases because the cutoff energy of 270 eV set by the interaction laser intensity prevents further extension of the plateau region. Thus, the HH intensity reaches a maximum at 250 eV. The measured HH spectrum is in sharp contrast to the conventional plateau of HH and clearly shows that the ALC is achieved by phase matching. The generation of the water window wavelength HH from the neutral Ne medium has been clearly demonstrated. The inset of Fig. 2 shows the measured far-field spatial profile of the water window x ray (290–310 eV). We directly obtained the spatial profile of the water window HH beam using a two-dimensional detector. The beam divergence was measured and had a 7 mrad full width at half maximum with a Gaussian profile. This good beam quality also indicates that the phase matching is substantially satisfied along the propagation axis of the pump pulse. Moreover, this 2D image ensures that our coherent water window source will be useful for acquiring 2D diffraction images.

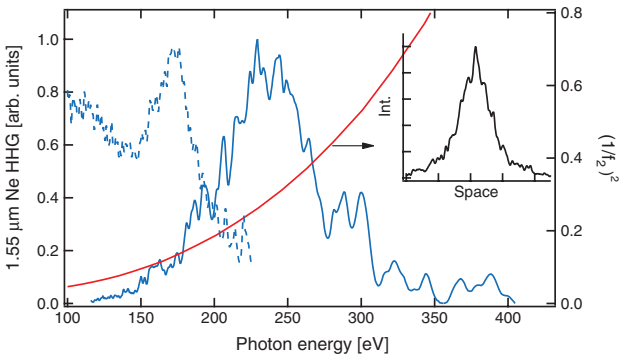

FIG. 2 (color). Measured harmonic spectra from neutral Ne and evolution of the square of the reciprocal of imaginary component f_2. The solid blue line and the dashed blue line (left axis) correspond to the Ne spectrum obtained with a 2400 grooves/mm grating and a 1200 grooves/mm grating, respectively. Both HH spectra are normalized to the peak intensity. The inset shows the far-field spatial profile of the water window x ray (280–310 eV) obtained from neutral Ne gas. Since a toroidal mirror is not set in front of the spectrometer, we can directly observe the spatial profile of the HH beam (see inset of Fig. 3).

We further explored the generation of HH under a neutral-medium condition by changing the nonlinear medium from Ne to He with the aim of obtaining a higher photon energy. Figure 3 shows the measured He HH spectra driven by a 1.55 μm pulse with a focusing intensity of 5.5×10^{14} W/cm^2, which is obtained with a 2400 grooves/mm grating. The pump energy, beam di-

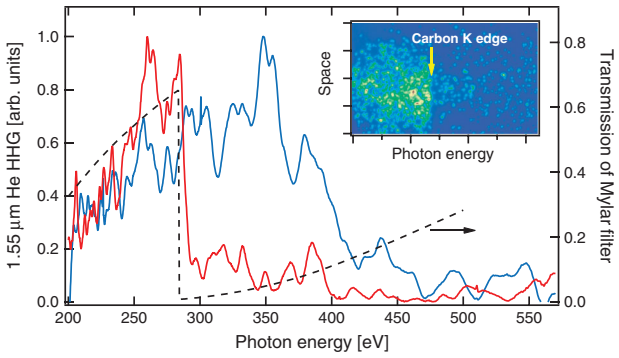

FIG. 3 (color). Measured harmonic spectra from neutral He. These spectra (left axis) are obtained with a 2400 grooves/mm grating. The red line and the blue line, respectively, correspond to the spectra with and without a 1-μm-thick Mylar filter ($C_{10}H_8O_4$). Both HH spectra are normalized to the peak intensity. The inset depicts a 2D HH spectrum image with a 1-μm-thick Mylar filter on a microchannel plate. This image is obtained by the accumulation of 1000 shots.

ameter, and backing pressure are 4.5 mJ, 15 mm, and 40 atm, respectively. We can clearly see the carbon K edge on the 2D HH spectral image by inserting a Mylar filter. Although the HH intensity above the carbon K edge gradually increases with the He gas pressure, we cannot determine the optimum gas pressure because of the limitation of the backing pressure of the gas jet. The measured HH intensity does not change significantly over a wide spectral region from 200 to 350 eV, although the absorption coefficient of He at 350 eV is one order magnitude larger than that at 200 eV. This dependence indicates that the medium condition is not fully optimized for the ALC. Here, we emphasize that the yield of He HH at the carbon K edge is two orders of magnitude lower than that of Ne HH. The maximum HH photon energy attained is 450 eV, which is the highest photon energy ever reported under a neutral-medium condition.

Taking our previous experimental results into account [30], we can design a water window high harmonic source for imaging live cells, because our proposed method has the advantage that the HH output yield can be scaled by increasing the harmonic emission size [8]. In a previous experiment, the CE of the Ne harmonic yield at 100 eV driven by a 0.8 μm laser was measured to be 2×10^{-7} [30]. When we apply the scaling formula $\lambda_0^{-5}(1/f_2)^2$, where the first term indicates the driving wavelength dependence of the HH yield [20,24] and the second term is the effect of the medium's absorption, we estimate the CE to be 6×10^{-8} at 250 eV with a driving laser wavelength of 1.55 μm. Since the evaluated photon yield for a Ne HH yield of approximately 2.5×10^6 photons/shot gives a CE of 5×10^{-8} at 250 eV in the present experiment, the HH output yield for neutral Ne can be accurately predicted by the above scaling formula. To obtain a sufficient harmonic yield around the water window region, the pump pulse wavelength should be extended to 1.65 μm because the maximum intensity of the Ne HH shifts to 300 eV. Consequently, a CE of 6.5×10^{-8} is estimated for a 300 eV HH driven with a 1.65 μm laser using the scaling formula. Using the estimated CE, we can obtain a single-shot fluence of 50 mJ/cm^2 over a 5×5 μm^2 area by upgrading the IR laser system to a pulse energy of 200 mJ and extending the focusing length to 5 m. This x-ray fluence is sufficient for obtaining a single-shot cell image by contact microscopy [31] with sub-100 nm spatial and sub-10 fs temporal resolutions. However, if we consider the HH loss due to focusing optics, we should further increase the output yield. The use of driving laser wavefront correction with a deformable mirror can improve the conversion efficiency by a factor of 2–3 [30]. Although our estimation is based on a single harmonic order, a bundle of several harmonic orders can be used for microscopy, which greatly increases the effective output fluence.

In summary, we have proposed the efficient phase-matched HHG of water window soft x ray using an IR laser pulse. Our proposed procedure for generating the water window x ray is efficient and scalable in output yield. By using our concept, we successfully obtained the high conversion efficiency and good beam quality water window HH beams under neutral phase-matched condition. The experimental results also give us the precept of design parameter for a single-shot cell image by contact microscopy. We believe that the presented method paves the way for the generation and application of intense ultrafast coherent water window x rays.

The authors acknowledge Dr. M. Toyoda at the Institute of Multidisciplinary Research for Advanced Materials, Tohoku University for valuable discussions on x-ray microscopy and optics. K. L. I. gratefully acknowledges financial support by the PRESTO program of the JST. This study was financially supported by a grant from the Research Foundation for Opto-Science and Technology.

*ejtak@riken.jp

[1] C. Spielmann *et al.*, Science **278**, 661 (1997)
[2] Z. Chang *et al.*, Phys. Rev. Lett. **79**, 2967 (1997).
[3] M. Hentschel *et al.*, Nature (London) **414**, 509 (2001).
[4] T. Sekikawa *et al.*, Nature (London) **432**, 605 (2004).
[5] G. Sansone *et al.*, Science **314**, 443 (2006).
[6] P. Tzallas *et al.*, Nature (London) **426**, 267 (2003).
[7] Y. Nabekawa *et al.*, Phys. Rev. Lett. **96**, 083901 (2006).
[8] E. J. Takahashi *et al.*, IEEE J. Sel. Top. Quantum Electron. **10**, 1315 (2004).
[9] In this Letter, a neutral condition means the effects of ionization are neglected during the duration of the laser pulse.
[10] P. B. Corkum, Phys. Rev. Lett. **71**, 1994 (1993).
[11] A. Paul *et al.*, Nature (London) **421**, 51 (2003).
[12] M. Zepf *et al.*, Phys. Rev. Lett. **99**, 143901 (2007).
[13] J. Seres *et al.*, Nature Phys. **3**, 878 (2007).
[14] E. A. Gibson *et al.*, Science **302**, 95 (2003).
[15] E. Seres *et al.*, Phys. Rev. Lett. **92**, 163002 (2004).
[16] B. Shan and Z. Chang, Phys. Rev. A **65**, 011804 (2001).
[17] V. S. Yakovlev *et al.*, Opt. Express **15**, 15351 (2007).
[18] K. L. Ishikawa *et al.*, Phys. Rev. A **75**, 021801(R) (2007).
[19] E. J. Takahashi *et al.*, Phys. Rev. Lett. **99**, 053904 (2007).
[20] K. Schiessl *et al.*, Phys. Rev. Lett. **99**, 253903 (2007).
[21] E. Constant *et al.*, Phys. Rev. Lett. **82**, 1668 (1999).
[22] B. L. Henke *et al.*, At. Data Nucl. Data Tables **54**, 181 (1993).
[23] P. Colosimo *et al.*, Nature Phys. **4**, 386 (2008).
[24] J. Tate *et al.*, Phys. Rev. Lett. **98**, 013901 (2007).
[25] E. J. Takahashi *et al.*, Appl. Phys. Lett. **93**, 041111 (2008).
[26] N. Nakano *et al.*, Appl. Opt. **23**, 2386 (1984).
[27] M. V. Amosov *et al.*, Zh. Eksp. Teor. Fiz. **91**, 2008 (1986).
[28] J. Sere *et al.*, New J. Phys. **8**, 251 (2006).
[29] S. Semushin and V. Malka, Rev. Sci. Instrum. **72**, 2961 (2001).
[30] E. J. Takahashi *et al.*, Appl. Phys. Lett. **84**, 4 (2004).
[31] T. Tomie *et al.*, Science **252**, 691 (1991).
[32] http://physics.nist.gov/PhysRefData/FFast/html/form.html.